Journal of Turbulence, 2014
Vol. 16, No. 1, 15–25, http://dx.doi.org/10.1080/14685248.2014.948628

Collision rate for suspensions at large Stokes numbers – comparing Navier–Stokes and synthetic turbulence

Michel Voßkuhle[a], Alain Pumir[a,b*], Emmanuel Lévêque[a,c] and Michael Wilkinson[d]

[a]*Laboratoire de Physique, ENS de Lyon and CNRS, Lyon, France;* [b]*Max-Planck Institute for Dynamics and Self-Organisation, Göttingen, Germany;* [c]*Laboratoire de Mécanique des Fluides et d'Acoustique, Ecole Centrale de Lyon and CNRS, Lyon, France;* [d]*Department of Mathematics and Statistics, The Open University, Walton Hall, Milton Keynes, United Kingdom*

(*Received 24 February 2014; accepted 20 July 2014*)

The use of simplified models of turbulent flows provides an appealing possibility to study the collision rate of turbulent suspensions, especially in conditions relevant to astrophysics, which require large timescale separations. To check the validity of such approaches, we used a direct numerical simulation (DNS) velocity field, which satisfies the Navier–Stokes equations (although it neglects the effect of the suspended particles on the flow field), and a kinematic simulation (KS) velocity field, which is a random field designed so that its statistics are in accord with the Kolmogorov theory for fully-developed turbulence. In the limit where the effects of particle inertia (characterised by the Stokes number) are negligible, the collision rates from the two approaches agree. As the Stokes number St increases, however, we show that the DNS collision rate exceeds the KS collision rate by orders of magnitude. We propose an explanation for this phenomenon and explore its consequences. We discuss the collision rate R for particles in high Reynolds number flows at large Stokes number, and present evidence that $R \propto \sqrt{\mathrm{St}}$.

Keywords: collisions; kinematic simulation; caustics; planet formation; rainfall

1. Introduction

A significant amount of work has been devoted in recent years to the determination of the collision rate of small particles suspended in a turbulent gas. This was primarily motivated by attempts to understand rainfall from warm cumulus clouds [1, 2], which depends upon collisions of microscopic water droplets. Another motivation comes from the efforts to model planet formation [3] involving aggregation of dust grains in turbulent circumstellar accretion discs. Collisions are also important in determining the properties of particle-laden turbulent flows such as snow avalanches and sandstorms [4].

The calculation of collision rates is a complex problem. It was appreciated early on that collision rates strongly depend on the inertia of the suspended particles, an effect which can be characterised by the Stokes number:

$$\mathrm{St} = \frac{\tau_\mathrm{p}}{\tau_\mathrm{K}} \tag{1}$$

*Corresponding author. Email: alain.pumir@ens-lyon.fr

where τ_p is the timescale for particle velocities to relax to the ambient flow, and τ_K is the Kolmogorov timescale: $\tau_K \equiv (\nu/\epsilon)^{1/2}$, with ϵ the rate of dissipation per unit mass and ν the kinematic viscosity of the fluid. For $St \ll 1$, particles are advected by the fluid, and collisions are the result of shear. The small St limit is particularly relevant to the problem of rain initiation [1]. When $St \gg 1$, the inertia of the particles allows them to move relative to the surrounding fluid. Two very different physical situations may occur when St is large. Turbulent flows are characterised by a large range of spatial and temporal scales. The timescale of eddies of scale l is of the order of $t_0 \sim (l^2/\epsilon)^{1/3}$. The ratio between the timescale of the largest eddies, T_L, and of the smallest eddies, τ_K, is known to be $T_L/\tau_K \approx 0.08\mathrm{Re}_\lambda$ [5], where Re_λ is the Taylor microscale Reynolds number. In very turbulent flows, relevant to astrophysical problems,

$$1 \ll St \ll T_L/\tau_K \tag{2}$$

a condition expressing that the largest eddies have a longer timescale than τ_p. The other case, $\tau_p > T_L$ is likely to probe a very different physical regime. Reliably determining the collision rate with condition (2) requires simulation of flows with a very large range of spatial and temporal scales, a very demanding endeavour.

The most realistic evaluation of the collision rate is obtained by using direct numerical simulation (DNS), where the velocity field satisfies the Navier–Stokes equations (to within numerical errors). There is a substantial literature on DNS collision rates, some notable contributions are [6–11]. It is, however, notoriously difficult to perform well-controlled DNS studies at very large values of the Reynolds number, Re, because the grid size, which determines the ratio of the integral scale to the Kolmogorov scale, is limited to numbers of order $(10^3)^3$. For most purposes, DNS calculations with this resolution provide a good approximation to the $\mathrm{Re} \to \infty$ limiting behaviour. The exception, however, occurs when we consider processes which probe long timescales in the flow, as effectively imposed by condition (2).

An alternative approach to DNS, consisting in using a randomly fluctuating velocity field whose properties mimic those of turbulent flows, has two potential advantages. An attractive feature is that if the statistics of the velocity field are known, it may be possible to compare with analytical theories. The principal benefit is that a random vector field requires fewer numerical operations and allows simulations with a larger range of scales, containing long-lived eddies. One especially refined version of the random velocity field approach is termed kinematic simulation (KS) [12]. The KS velocity field contains several parameters, which introduces uncertainties into the collision rates. Few studies use KS to determine collision rates [13, 14]. In particular, we are not aware of earlier work directly comparing the collision rates predicted by the DNS and KS approaches.

An enticing approach could consist in combining the use of both DNS and KS velocity fields. Using the collision rate determined from DNS at intermediate Stokes numbers, $St \lesssim 1$, one could adjust the parameters of the KS velocity field to match the DNS collision rate. Then at large Stokes numbers, the collision rate could be obtained from KS simulations.

We attempted to use this approach to investigate collision rates at large Stokes numbers. Unexpectedly, we found that the approach is not viable, because at Stokes number $St \lesssim 1$, the DNS collision rates exceed the KS rates by a large factor, which cannot be reduced by adjusting parameters of the KS simulation. Figure 1 illustrates the comparison between collision rates evaluated using the two approaches: they agree only at very small Stokes

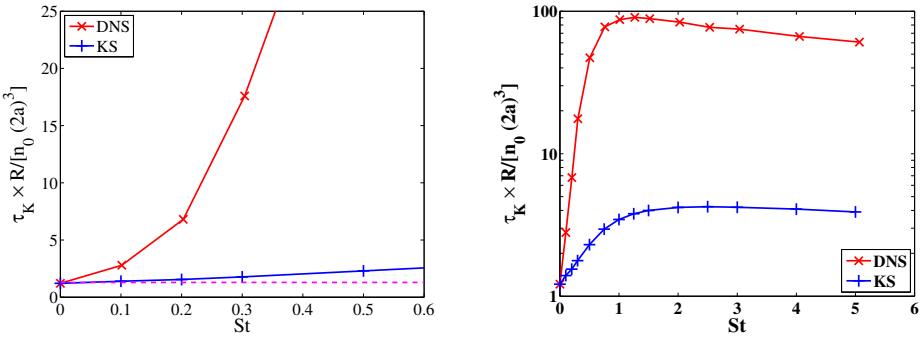

Figure 1. Comparison of collision rates evaluated using DNS and KS velocity fields as a function of the Stokes number. The KS were performed with the parameter λ, defined in Equation (11), fixed at 0.5. (a) linear scale, shows that the collision rates agree at small Stokes number, (b) logarithmic scale. The predictions of DNS and KS agree only in the limit $\mathrm{St} \to 0$, and coincide with the prediction of [18], shown by the dotted line. At values of the Stokes number larger than $\mathrm{St} \gtrsim 0.3$, the collision rate R determined with the KS flow is smaller by more than one order of magnitude compared to the collision rate obtained in DNS.

number.

In this paper, we document this observation, propose an explanation for the discrepancy, and discuss the problem of making a quantitatively accurate estimate for the collision rate at large Stokes numbers. We also remark that there is a similar discrepancy between DNS and KS simulations in the clustering behaviour of particles.

2. Theoretical background

In this section, we briefly review the available understanding of the collision rate in turbulent suspensions. The main result, (7), expresses the collision rate as a sum of two contributions, originating from two different effects induced by the particle inertia. In the limit of large Stokes numbers, under condition (2), the limiting behaviour of the collision rate is predicted to be given by a simple analytic expression, (8).

For a suspension of spherical particles of radius a, the rate of collision of a given particle with any other particle may be written

$$R = 2\pi n_0 a^2 \langle w \rangle \tag{3}$$

where n_0 is the number density of particles, and $\langle w \rangle$ is a suitably defined average of the relative velocity of two particles when their separation is equal to $2a$ [7, 8]. The total collision rate per unit volume in the suspension is simply obtained by multiplying R by $n_0/2$. The collision rates have been investigated by a succession of authors using simulations where particles move independently under the simplified Gatignol/Maxey–Riley equations of motion [15, 16].

$$\dot{\boldsymbol{r}} = \boldsymbol{v}\,, \quad \dot{\boldsymbol{v}} = \frac{1}{\tau_\mathrm{p}}[\boldsymbol{u}(\boldsymbol{r}, t) - \boldsymbol{v}] \tag{4}$$

where

$$\tau_\mathrm{p} = \frac{2}{9}\frac{a^2}{\nu}\frac{\rho_\mathrm{p}}{\rho_\mathrm{f}} = \frac{2}{9}\frac{\rho_\mathrm{p}}{\rho_\mathrm{f}}\frac{a^2}{\eta^2}\tau_\mathrm{K} \tag{5}$$

is the particle relaxation time, determined from Stokes formula for the drag on a moving sphere, ρ_f and ρ_p being respectively the fluid and particle densities, and $\eta = (\nu^3/\epsilon)^{1/4}$ is the Kolmogorov length. These equations of motion depend on the velocity $\boldsymbol{u}(\boldsymbol{r}, t)$ of the surrounding fluid at the position $\boldsymbol{r}$ of the particle and are valid in the limit where the suspended particles are very small and very dense: $\rho_\mathrm{p}/\rho_\mathrm{f} \gg 1$. Most works have defined the collision rate as being the rate for the separation between non-interacting particles decreasing past $2a$. In practice, this 'ghost collision approximation' may overestimate the collision rate, because collisions may be inhibited by lubrication effects, and because multiple collisions should not be counted if particles adhere, coalesce, or react on contact [17]. In this work, we use the ghost collision approximation, because our objective is to isolate the effects of turbulence from other phenomena.

The early work of Saffman and Turner [18] considers the case where the Stokes number is small, so that the suspended particles are advected with the flow. In this limit, collisions occur due to shearing motion, so that $\langle w \rangle \sim a/\tau_\mathrm{K}$. Saffman and Turner showed that if the 'ghost collision' criterion is used as the definition of the collision rate, then for $\mathrm{St} \ll 1$ the rate of collision of a given spherical particle of radius a with any other particle is

$$R_\mathrm{ST} = \sqrt{\frac{8\pi}{15}}\frac{n_0(2a)^3}{\tau_\mathrm{K}}\,. \tag{6}$$

This expression is exact in the limit as $\mathrm{St} \to 0$, and in this paper Equation (6) will be used as a benchmark for comparing collision rates in turbulent flow.

When the Stokes number is not small, the inertia of the suspended particles allows them to follow trajectories which differ from fluid streamlines. This brings two additional effects into play, which can substantially increase the collision rate. The first mechanism which has been proposed to enhance the collision rate [6] is the tendency for inertial particles in turbulent flows to exhibit a clustering effect, known as preferential concentration [19]. This has the effect of introducing an additional factor in Equation (6): the collision rate is multiplied by $g(2a)$, where $g(r)$ is the radial distribution function describing the clustering effect. The other mechanism for enhancing the collision rate is that the particle velocity can become multivalued, due to the formation of caustic folds in the phase-space of the suspended particles [20], and this effect can lead to an enhancement of the collision rate [21]. The same mechanism has also been described as a 'sling effect', where particles collide because they are centrifuged out of vortices [22].

These inertial effects are included by adopting the following model for the collision rate

$$R = R_\mathrm{ST}\, g(2a) + n_0 a^2 u_\mathrm{K}\, f(\mathrm{St}, \mathrm{Re}) \tag{7}$$

where f is a function of the Stokes number and the Reynolds number. The factor $g(2a)$ accounts for the enhancement of the advective collision mechanism by the preferential concentration effect, as has been explained above. The second term in the right-hand side of Equation (7) describes the collisions of particles whose velocities differ significantly

from the flow velocity, so that their relative velocity is proportional to u_K, i.e., does not vanish in the limit of very small particle separation, and therefore, for small, dense particles greatly exceeds a/τ_K. The function $f(\mathrm{St}, \mathrm{Re})$ approaches zero rapidly as $\mathrm{St} \to 0$, so that Equation (6) is valid in this limit. The theoretical basis for Equation (7) was set out in [21–23], and recent DNS simulations at moderate Stokes numbers ($\mathrm{St} \leq 5$) [24] lend strong support to its validity. In particular, simulations do show a marked increase in the collision rate when St is of order unity, and the DNS simulations are consistent with theoretical expectations, at least at moderate Stokes numbers.

As explained in the introduction, the collision rate at very large Stokes numbers is an important issue for models of planet formation, and may also be significant for models of particle-laden geophysical flows. Different lines of argument, explicitly using condition (2) [25, 26] indicate that

$$f(\mathrm{St}, \infty) \sim K\mathrm{St}^{1/2} \tag{8}$$

as $\mathrm{St} \to \infty$. Providing numerical evidence to establish the validity of Equation (8), and to determine the coefficient K would lead to an explicit and reliable parametrisation of the collision rate in the important limit of large Stokes numbers.

However, DNS studies are limited to quite small values of St, and it has not been possible to see conclusive evidence that $f(\mathrm{St}, \infty) \propto \sqrt{\mathrm{St}}$, or to determine the coefficient K in Equation (8). The difficulty in investigating the validity of Equation (8) using directly DNS is one of the primary reasons to look for alternative numerical methods, based on the simplified KS flow models.

3. Numerical studies comparing DNS and KS

We used a standard pseudo-spectral code to determine the solutions of the Navier–Stokes equations:

$$\begin{aligned} \partial_t \boldsymbol{u} + (\boldsymbol{u} \cdot \nabla)\boldsymbol{u} &= -\nabla p + \nu \nabla^2 \boldsymbol{u} + \boldsymbol{f} \\ \nabla \cdot \boldsymbol{u} &= 0 \end{aligned} \tag{9}$$

in a triply periodic domain of size 2π. Here, we assume that the fluid density ρ_f is equal to 1. The term $\boldsymbol{f}$ corresponds to a forcing term, acting at the scale of the box. The code is fully dealiased. We used $N = 256$ modes, and a corresponding discretisation of the spatial domain with 384 points. The DNS results presented here are from the same set of simulations as those in reference [17].

Figure 2, which shows the averaged energy spectrum of the turbulent flow simulated, multiplied by $\epsilon^{-2/3}k^{5/3}$ provides a way to judge the intensity of the turbulence, as well as the quality of our numerical resolution. The compensated spectrum is essentially constant over a range of scales larger than a decade, for $1 \leq k \leq 0.2\eta^{-1}$. Thus, our simulations exhibit a moderate range of inertial scales, characteristic of turbulent flows. The corresponding Reynolds number here is $\mathrm{Re}_\lambda = 130$. Although larger Reynolds numbers (and correspondingly wider range of scales) can now be simulated [27, 28], our objective here is to cover a large range of values of Stokes numbers, and to determine accurately a collision rate, which requires long integration times.

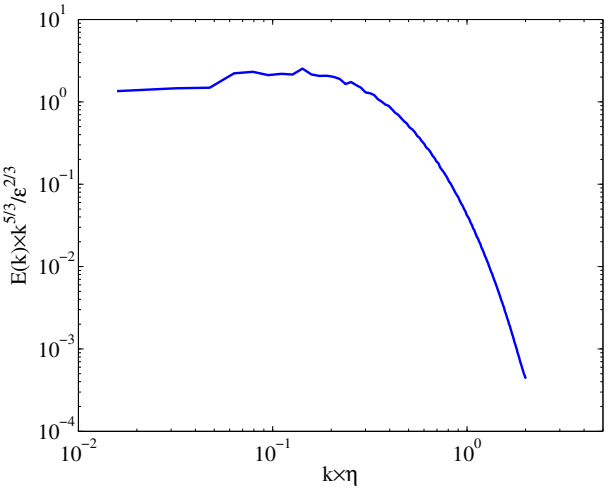

Figure 2. (Colour online). Spectrum of the turbulent flow used to determine the collision rate, multiplied by $\epsilon^{-2/3} \times k^{5/3}$. The compensated spectrum exhibits an inertial range of scales, over a range of scales of order ~ 10, where $E(k)/\epsilon^{2/3}k^{5/3} \approx C_{\mathrm{K}}$, with $C_{\mathrm{K}} \approx 1.55$ (the Kolmogorov constant).

The parameters of our turbulent velocity field were fixed for all of our simulations. In the DNS simulations reported here, we set $\rho_{\mathrm{p}} = 10^3$ throughout, and varied the Stokes number by varying the particle radius a, using Equation (5).

It appears to be possible to study the collision rate at large Stokes number by replacing the DNS velocity field with a KS velocity field, because generating the synthetic field requires fewer numerical operations, and allows investigations of larger systems.

The details of how we implemented this KS velocity field model as well as the chosen parameters are described in [13], and are summarised briefly here. The velocity field is

$$\boldsymbol{u}(\boldsymbol{r},t) = \sum_{n=1}^{\mathcal{N}} \Big(\boldsymbol{a}_n \cos(\boldsymbol{k}_n \cdot \boldsymbol{r} + \omega_n t) + \boldsymbol{b}_n \sin(\boldsymbol{k}_n \cdot \boldsymbol{r} + \omega_n t) \Big) \tag{10}$$

where $\boldsymbol{k}_n \cdot \boldsymbol{a}_n = \boldsymbol{k}_n \cdot \boldsymbol{b}_n = 0$ (to ensure that the field is incompressible) and the vectors $\boldsymbol{a}_n$ and $\boldsymbol{b}_n$ are chosen at random, with the variances of their elements prescribed so that the velocity field has a spectral density which is in agreement with the Kolmogorov law: $E(\boldsymbol{k}) = E_0 |\boldsymbol{k}|^{-5/3}$. The coefficient E_0, chosen here to be $E_0 = 1.0$, determines the rate of dissipation ϵ, by using the well-known analytic form of the velocity spectrum in the inertial range: $E(k) = C_{\mathrm{K}} \epsilon^{2/3} k^{-5/3}$, where C_{K}, the Kolmogorov constant, is $C_{\mathrm{K}} \approx 1.5$. The choice of the upper and lower cutoff for the wavevectors determines the Kolmogorov length η and the lengthscale of the largest eddies L, respectively. All results shown in this work were obtained at a moderate scale ratio of $L/\eta = 64$ and the number of modes was fixed at $\mathcal{N} = 109$. The choice of a relatively moderate value of L/η, comparable to the range of inertial range obtained in our numerical simulations, is appropriate to directly compare the predictions of DNS and KS concerning the collision rate.

The frequencies ω_n in Equation (10) are determined by the relation between lengthscale and eddy turnover time which is implied by Kolmogorov's dimensional analysis:

$$\omega_n = \lambda \sqrt{|\boldsymbol{k}_n|^3 E(\boldsymbol{k})} \tag{11}$$

where λ is a dimensionless coefficient, which determines the phase velocity of the modes. The value of the coefficient λ is not predicted by the Kolmogorov theory. It determines the Kubo number of the flow: $\mathrm{Ku} = u_0\tau/\xi$, where u_0, τ and ξ are, respectively, velocity, length and timescales associated with the smallest eddies in the flow. The Kolmogorov theory identifies these quantities as being proportional to u_K, τ_K and η, respectively. Dimensional arguments then establish that Ku is of order unity, but the precise value of λ is unknown.

As with the DNS simulations, the parameters of the KS velocity field were fixed, and the Stokes number was varied by changing the particle radius and applying Equation (5). As for the DNS simulations, we used $\rho_\mathrm{p}/\rho_\mathrm{f} = 10^3$. In the case of the KS simulations, the Stokes number is computed from η, rather than from ν. There is a degree of arbitrariness in the way η is defined via the upper cutoff wavenumber, which could be compensated for by introducing a multiplicative coefficient in the final term of Equation (5). Our results indicate that such adjustments would not be of any use, as the differences between DNS and KS are qualitatively too large.

These considerations lead to the following proposal: that the KS simulation can be 'calibrated' against DNS simulations to determine the appropriate value for λ: that is, the value of λ should be chosen to make the KS collision rate match the DNS rate as closely as possible at small values of the Stokes number, where reliable DNS data can be determined. The collision rate could then be extrapolated to high values of the Stokes number using KS simulations.

We tested this approach, using the methods described in [17, 24] to compute the DNS collision rate. The procedure, however, was found to fail: the DNS collision rate rapidly becomes much larger than the KS collision rate as the Stokes number St increases. The two collision rates are compared in Figure 1 using both linear and logarithmic scales. Here a value of $\lambda = 0.5$ was used for the KS. However, the discrepancy observed numerically is so large that no adjustment of λ can make the two collision rates agree exactly, except in the limit as $\mathrm{St} = 0$, where the prediction of Saffman and Turner becomes exact in the 'ghost-collision' approximation. This is illustrated in Table 1, which shows the dependence of the normalised collision rate, $R\tau_\mathrm{K}/(2a)^3$ on λ, at the value $\mathrm{St} = 1.5$. The normalised collision rate is found to be a decreasing function of λ. However, when λ decreases from $\lambda = 0.5$, which is the value taken in most simulations, to $\lambda = 0.01$, the normalised collision rate, $R\tau_\mathrm{K}/(2a)^3$ increases by less than a factor of 2 at $\mathrm{St} = 1.5$. This is insufficient to correct for the difference, clearly seen in Figure 1, between the DNS and KS results at $\lambda = 0.5$. Increasing λ to the value 2, on the other hand decreases the collision rate by a factor ~ 1.5. We checked that these conclusions, based on the data shown in Table 1, extend to the entire range of Stokes numbers investigated here.

The DNS and KS collision rates agree exactly in the limit $\mathrm{St} \to 0$ because R_ST can be expressed in terms of the expectation value of the trace of the square of the strain-rate matrix. Since this quantity depends only upon the spatial derivatives of the velocity field, and not

Table 1. The dependence of the collision rate, normalised by $\tau_\mathrm{K}/n_0(2a)^3$, on the parameter λ (defined by Equation (11)), at a fixed value of the Stokes number ($\mathrm{St} = 1.5$) and of the ratio of scales for $L/\eta = 64$. From the DNS results, one would expect $R\tau_\mathrm{K}/n_0(2a)^3 = 88.6 \pm 1$.

λ	0.01	0.1	0.5	1.0	2.0
$R\tau_\mathrm{K}/n_0(2a)^3$	6.3	5.7	4.0	3.1	2.6

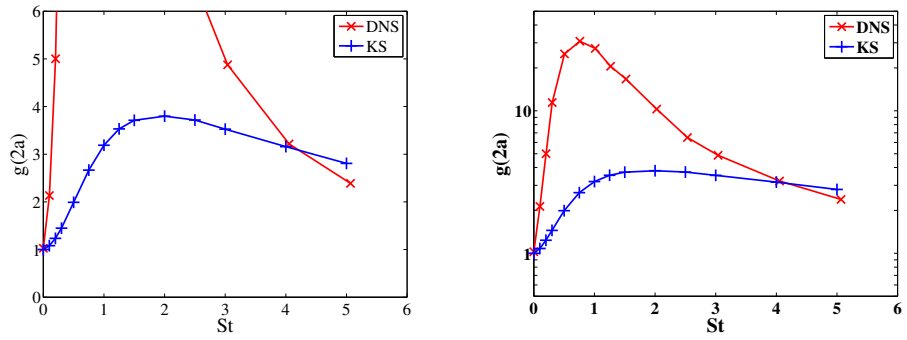

Figure 3. Comparison of the preferential concentration, measured by the pair correlation function $g(2a)$, as a function of the Stokes number: (a) linear scale, shows that the preferential concentration effect is not present at small Stokes number, (b) logarithmic scale, shows that the preferential concentration in the KS flow field is too low by more than one order of magnitude at larger Stokes number. The data shown here is from the same simulations as in Figure 1.

upon its kinematics, the KS collision rate for $\mathrm{St} \to 0$ is asymptotic to R_{ST}, independent of the value of λ.

We also compared the preferential concentration effect for the two velocity fields, finding that the preferential concentration is much weaker in KS velocity fields, as compared to the equivalent DNS field. This is illustrated in Figure 3.

4. Discussion

Our numerical studies indicate that seeking to extrapolate numerical estimates of collision rates to large Stokes numbers using KS velocity fields is not a viable program, because the KS data become very inaccurate as the Stokes number St increases past a value of the order $\mathrm{St} \gtrsim 0.1$, see Figure 1.

This observation is also significant for theoretical discussions of collision rates, which consider the rate of collision processes in randomly defined velocity fields. The KS velocity field is just a specific example of a random velocity field. Our work shows that caution must be applied when interpreting the results of these calculations.

We should consider why the KS model performs so badly. The minor quantitative difference between the energy spectra in the KS and in the DNS flows can hardly explain the discrepancy in the predicted collision rate between the two flows, since the effect of low-amplitude, high-wavenumber modes, with a large frequency, will have only a minor impact on particles with Stokes numbers $\mathrm{St} \gtrsim 1$. Two other reasons can be proposed to explain the very large discrepancy observed when studying numerically the collision rates in DNS and KS. The most plausible mechanism is a failing of the KS approach known as the 'sweeping effect' which was already mentioned in the original paper where the method was introduced [12]. In the realistic DNS model, both the particles and the smaller eddies are swept along by the larger eddies. In the KS simulations, however, the particles are swept but the small 'eddies' do not move. This means that the fluctuations caused by the small eddies (those which create the relative velocities) have a reduced correlation time (when viewed by the particles) and are therefore less effective. The caustics [20], inducing a multivalued velocity distribution of the particles [22], and constituting the predominant mechanism

for increasing the collision rate [24], are generated at a slower rate in the case of the KS velocity field, with a consequent reduction of the collision rate. As the integral size scale of the simulation is increased, the velocity of the particles relative to the eddies increases, so that the discrepancy in the collision rate increases. This mechanism is, therefore, able to account for the gross errors seen in the KS collision rate simulations.

The other possible mechanism for the discrepancy concerns the well-documented existence of structures in turbulent flows, which induce large, non-Gaussian, fluctuations of the velocity field gradients (vorticity and strain rate, see [28]). Their role, however, is difficult to quantify precisely.

It is interesting to notice that, while the version of KS implemented here, as well as in many other studies, leads to an incorrect sweeping of the small eddies by the flow, the issue of properly incorporating the sweeping in a simplified model had been discussed in the original paper of [12]. The ideas developed in [12] may help to devise a practically tractable version of the KS, permitting to better treat the sweeping effect.

Random flow field models which use single-scale velocity fields have been very successful in explaining the qualitative features of the role of caustics in enhancing collision rates [21, 29]. They have also been shown to be able to give quantitatively correct results in describing preferential concentration [30]. Our results indicate that attempts to improve upon the predictive ability of random flow models for turbulence by incorporating the multi-scale aspect of the flow seem to be unsuccessful. The reason for this failure can be attributed to the lack of sweeping of the small eddies by the large eddies in the KS model. This very important difference of the KS flow, in comparison to DNS has been shown to lead to different predictions [31]. In particular, it has been qualitatively noticed that preferential concentration is reduced in KS [32]. We find that even in the range of Stokes number $\mathrm{St} \gtrsim 1$, where the enhancement of the collision rate is not so much due to preferential concentration, but rather to the caustics effect [24], the KS model seriously underestimates the collision rates.

The evaluation of the collision rate in turbulence at large Stokes and Reynolds remains a significant open problem. The results presented here indicate that only DNS evaluations should be considered reliable. The best approach is to utilise DNS data at the largest Stokes number for which a DNS collision rate has been observed to be substantially independent of the Reynolds number. We used data from a high resolution study of collisions in turbulent flows by Rosa *et al.*, [10], together with our own data from [24]. In accord with arguments in [25, 26] and with Equations (7) and (8) above, we fitted a collision rate proportional to $\sqrt{\mathrm{St}}$. The data plotted in Figure 4 indicate that the collision rate for turbulence with very high Reynolds numbers is

$$R \approx K n_0 a^2 u_{\mathrm{K}} \sqrt{\mathrm{St}}\,, \quad K = 50, \tag{12}$$

for large values of the Stokes number, with the plateau being reached by $\mathrm{St} \approx 1.2$. Note that, while the curves show a decrease for larger values of St, they appear to approach a plateau as the Reynolds number increases. The position of the plateau and therefore the exact value of the constant K seem to depend (slightly) on the Reynolds number. However, until simulations at higher Reynolds number become available, Equation (12) is the best available estimate for the collision rate of monodisperse spherical particles at high Stokes number.

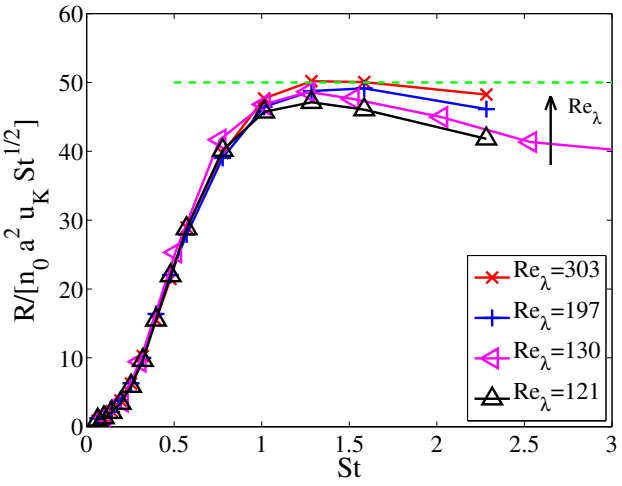

Figure 4. (Colour online). Plot of the collision rate R divided by $n_0 a^2 u_K \sqrt{\mathrm{St}}$, as a function of St. The curves appear to approach a plateau at large St as the Reynolds number increases, consistent with Equation (12). The data for $\mathrm{Re}_\lambda = 130$ are from [24], the other data are re-plotted from [10].

Acknowledgements

The authors acknowledge informative discussions with B. Mehlig, K. Gustavsson and L. Collins.

Funding

AP and EL have been supported by the grant 'TEC 2' from A.N.R. (ANR-12-BS09-0011-02). Computations were performed at the PSMN computing center at the Ecole Normale Supérieure de Lyon. MW and AP were supported by the EU COST action MP0806 'Particles in Turbulence'. AP acknowledges the support from the Alexander-von-Humboldt foundation.

References

[1] R.A. Shaw, *Particle-turbulence interactions in atmospheric clouds*, Annu. Rev. Fluid Mech. 35 (2003), pp. 183–227.
[2] W.W. Grabowski and L.-P. Wang, *Growth of cloud droplets in a turbulent environment*, Annu. Rev. Fluid Mech. 45 (2013), pp. 293–324.
[3] V.S. Safranov, *Evolution of the protoplanetary cloud and formation of earth and planets*, NASA Tech. Transl. F-677; Moscow, Nauka, 1969.
[4] S. Elghobashi, *On predicting particle-laden turbulent flows*, Appl. Sci. Res. 52 (1994), pp. 309–329.
[5] B.L. Sawford and P.K. Yeung, *Kolmogorov similarity scaling for one-particle Lagrangian statistics*, Phys. Fluids 23 (2011), 091705.
[6] S. Sundaram and L.R. Collins, *Numerical considerations in simulating a turbulent suspension of finite volume particles*, J. Comput. Phys. 124 (1996), pp. 337–350.
[7] S. Sundaram and L.R. Collins, *Collisions statistics in an isotropic particle-laden turbulent suspension. Part 1. Direct numerical simulations*, J. Fluid Mech. 335 (1997), pp. 75–109.
[8] L.P. Wang, A.S. Wexler, and Y. Zhou, *Statistical mechanical description and modelling of turbulent collisions of inertial particles*. J. Fluid Mech. 415 (2000), pp. 117–153.
[9] W.C. Reade and L.R. Collins, *Effect of preferential concentration on turbulent collision rates*, Phys. Fluids 12 (2000), pp. 2530–2540.
[10] B. Rosa, H. Parishani, O. Ayala, W.W. Grabowski, and L.P. Wang, *Kinematic and dynamic collision statistics of cloud droplets from high resolution simulations*, New J. Phys. 15 (2013), 045032.
[11] G. Falkovich and A. Pumir, *Sling effect in collisions of water droplets in turbulent clouds*, J. Atmos. Sci. 64 (2007), pp. 4497–4505.

[12] J.C.H. Fung, J.C.R. Hunt, N.A. Malik, and R.J. Perkins, *Kinematic simulation of homogeneous turbulence by unsteady random Fourier modes*, J. Fluid Mech. 236 (1992), pp. 281–318.
[13] L. Ducasse and A. Pumir, *Inertial particle collisions in turbulent synthetic flows: Quantifying the sling effect*, Phys. Rev. E 80 (2009), 066312.
[14] R.H.A. IJzermans, E. Meneguz, and M.W. Reeks, *Segregation of particles in incompressible random flows: Singularities, intermittency and random uncorrelated motion*, J. Fluid Mech. 653 (2010), pp. 99–136.
[15] M.R. Maxey and J.J. Riley, *Equation of motion for a small rigid sphere in a nonuniform flow*, Phys. Fluids 26 (1983), pp. 883–889.
[16] R. Gatignol, *The Faxen formulae for a rigid particle in an unsteady non-uniform Stokes flow*, J. Mec. Theor. Appl. 1 (1983), pp. 143–160.
[17] M. Voßkuhle, A. Pumir, E. Leveque, and M. Wilkinson, *Multiple collisions in turbulent flows*, Phys. Rev. E 88 (2013), 063008.
[18] P.G. Saffman and J.S. Turner, *On the collsion of drops in turbulent clouds*, J. Fluid. Mech. 1 (1956), pp. 16–30.
[19] M.R. Maxey, *The gravitational settling of aerosol particles in homogeneous turbulence and random flow fields*, J. Fluid Mech. 174 (1987), pp. 441–465.
[20] M. Wilkinson and B. Mehlig, *Caustics in turbulent aerorols*, Europhys. Lett. 71 (2005), pp. 186–192.
[21] M. Wilkinson, B. Mehlig, and V. Bezuglyy, *Caustics activation of rain showers*, Phys. Rev. Lett. 97 (2006), 048501.
[22] G. Falkovich, A. Fouxon, and M.G. Stepanov, *Acceleration of rain initiation by cloud turbulence*, Nature 419 (2002), pp. 151–154.
[23] K. Gustavsson and B. Mehlig, *Distribution of relative velocities in turbulent aerosols*, Phys. Rev. E 84 (2011), 045304.
[24] M. Voßkuhle, A. Pumir, E. Leveque, and M. Wilkinson, *Prevalence of the sling effect for enhancing collision rates in turbulent suspensions*, J. Fluid Mech. 749 (2014), pp. 841–852.
[25] H.J. Völk, F.C. Jones, G.E. Morfill, and S. Röser, *Collisions between grains in a turbulent gas*, Astron. Atrophys. 85 (1980), pp. 316–325.
[26] B. Mehlig, V. Uski, and M. Wilkinson, *Colliding particles in highly turbulent flows*, Phys. Fluids 19 (2007), 098107.
[27] T. Ishihara, T. Gotoh, and Y. Kaneda, *Study of high-Reynolds number isotropic turbulence by direct numerical simulation*, Ann. Rev. Fluid Mech. 41 (2009), pp. 165–180.
[28] P.K. Yeung, D.A. Donzis, and K.R. Sreenivasan, *Dissipation, enstrophy and pressure statistics in turbulence simulation at high Reynolds numbers*, J. Fluid Mech. 700 (2012), pp. 5–15.
[29] K. Gustavsson and B. Mehlig, *Relative velocities of inertial particles in turbulent aerosols*, J. Turbul. 15 (2014), pp. 34–69.
[30] M. Wilkinson, B. Mehlig, S. Östlund, and K.P. Duncan, *Unmixing in random flows*, Phys. Fluids 19 (2007), 113303.
[31] D.J. Thomson and B. Devenish, *Particle pair separation in kinematic simulations*, J. Fluid Mech. 526 (2005), pp. 277–302.
[32] L. Chen, S. Goto, and J.C. Vassilicos, *Turbulent clustering of stagnation points and inertial particles*, J. Fluid Mech. 553 (2006), pp. 143–154.